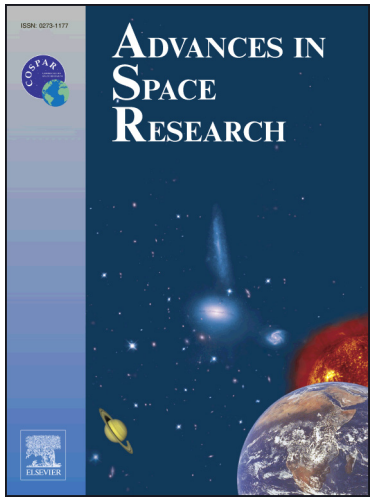

Analysis of the consequences of fragmentations in Low and Geostationary orbits

A. Rossi, H. Lewis, A. White, L. Anselmo, C. Pardini, H. Krag, B. Bastida Virgili

PII: S0273-1177(15)00375-0
DOI: http://dx.doi.org/10.1016/j.asr.2015.05.035
Reference: JASR 12278

To appear in: *Advances in Space Research*

Received Date: 25 March 2015
Revised Date: 6 May 2015
Accepted Date: 24 May 2015

Please cite this article as: Rossi, A., Lewis, H., White, A., Anselmo, L., Pardini, C., Krag, H., Bastida Virgili, B., Analysis of the consequences of fragmentations in Low and Geostationary orbits, *Advances in Space Research* (2015), doi: http://dx.doi.org/10.1016/j.asr.2015.05.035

Analysis of the consequences of fragmentations in Low and Geostationary orbits

A. Rossi*

IFAC-CNR, Via Madonna del Piano 10, 50019, Sesto Fiorentino, Italy

H. Lewis, A. White

Faculty of Engineering and the Environment, University of Southampton, Southampton SO17 1BJ, United Kingdom

L. Anselmo, C. Pardini

ISTI-CNR, 56124 Pisa, Italy

H. Krag, B. Bastida Virgili

ESA-ESOC Space Debris Office, DE-64293 Darmstadt, Germany

Abstract

The present distribution of intact objects is a good proxy to quantify the catastrophic collision risk and consequences in the coming decades. The results of a large number of long term simulations of the LEO environment perturbed by the collisional fragmentation of massive objects are used to identify the main driving parameters of the long term collisional evolution of the debris population and measure the danger represented by "typical" classes of space objects. An evaluation norm, able to highlight the differences between comparative long term evolution scenarios and to give a quantitative measure of the effects of specific parameters affecting the evolution, is devised. It is shown how, for collisional fragmentations in LEO, due to the highly stochastic evolution of the LEO environment, even the fragmentation of a massive spacecraft might not be able to alter the long term evolution of the LEO population beyond the intrinsic statistical variability associated

*Corresponding author
Email address: a.rossi@ifac.cnr.it (A. Rossi)

with the Monte Carlo procedure. Among the parameters determining the long term effects of a collisional fragmentation in LEO, a combination of mass and altitude of the event appears to be the driving factor. In GEO, the situation is different, and the addition of a massive fragmentation lives a signature on the environment that is detectable throughout the investigated time span, with the mass being the only factor important to asses the long term consequences of a collisional fragmentation.

Keywords: Space debris; Fragmentations; Long term evolution.

1. Introduction

The present distribution of intact objects is a good proxy to quantify the catastrophic collision risk and consequences in the coming decades. For this reason, it is important to understand the effects of selected "typical" collisional fragmentations on the long term evolution of the debris population, as a function of the main driving parameters, with the goal of measuring the danger represented by "typical" classes of space objects. To tackle this problem, the European Space Agency (ESA/ESOC) financed a contract, named *Assessment Study for Fragmentation Consequence Analysis for LEO and GEO Orbits* foreseeing a large number of long term simulations to analyze the effects on the circumterrestrial environment of many different collisional fragmentations.

All the long term simulations were performed using either SDM 4.2 (Rossi et al. , 2009) or DAMAGE (Lewis et al. , 2012). They are two well known long term evolution codes, developed in Italy (SDM) and in the United Kingdom (DAMAGE) in the last decades. The two codes allow a very detailed and accurate modelling of the debris environment in Earth orbit, taking into account all the main sources and sinks terms affecting the future evolution of the debris population. As a validation, the two models were subject to several international comparisons with similar software suites developed by other research groups and space agencies worldwide, both within the framework of the Inter-Agency Space Debris Coordination Committee((IADC) studies (Liou et al. , 2013) and also in the course of the study presented here. In the following, both results obtained with SDM 4.2 and with DAMAGE will be shown alternatively, where deemed significant.

2. The simulation strategy and the Reference scenario

The main simulation strategy consisted in comparing the long term evolution results of a Reference scenario with those of a number of scenarios where a number of different spacecraft were supposed to collisionally fragment in selected epochs. That is, in the long term runs, at the selected epochs a given spacecraft was "artificially" fragmented by a simulated collision and the clouds of fragments were added to the simulation. Comparing the long term evolution in the cases with and without the additional fragments generated by the artificially introduced fragmentation, the effect of the particular fragmentation on the environment was evaluated.

As a reference, a long term evolution scenario was simulated for a time span of 200 years. With Reference scenario, we mean that the traffic launch repeats an 8-year cycle representing the current launch pace, that is the new launched objects are inserted into orbits similar to those populated in the recent past. An 8-year operational lifetime is assumed for future spacecraft, no new explosions are considered and no avoidance maneuvers are performed. A post mission disposal scenario according to the 25-year rule is adopted, with a 60 % compliance to this rule. That is, given all the spacecraft that do not re-enter naturally in 25 years, only 60% of them are actually deorbited at end-of-life. The above assumptions are common to most of the recent studies of the long term evolution of the space debris population. As in most of the modelling works, there are of course uncertainties related to these assumptions, e.g. the traffic launch cannot be predicted accurately for 200 years in the future, as well as the solar activity, etc. Nonetheless the above assumptions represent good, standard hypotheses that are well suited to produce an "average" reliable future environment appropriate for the purpose of the present study. The Reference scenario was simulated with 50 Monte Carlo (MC) runs both with SDM and DAMAGE and the results were compared, in order to have a reliable Reference scenario against which the fragmentations cases could be compared. In all the simulation the objects larger than 10 cm are considered. Whereas particles smaller than 10 cm can, in some peculiar cases (i.e., small targets and high impact velocities), generate catastrophic fragmentations, it was observed in previous studies that the long term collisional evolution is mainly driven by the objects larger than 10 cm that can generate large debris clouds, upon fragmentation of large targets.

Figures 1-2 shows the main results for the Reference scenario. The left panel of Fig. 1 shows the average number of objects larger than 10 cm in

LEO with SDM (thick blue line) and DAMAGE (thick red line), along with the respective 1-sigma curves (thin lines). It can be noticed how the two codes give remarkably comparable results after the long term evolution, with both averages lying well within the 1-sigma bars of the other model. This gives a clear indication that the two models can be used alternatively in the course of the study, leading to comparable and reliable results. The small jump in the blue line around the year 2115 is due to a chance accumulation of large fragmentations happening around that epoch in a few MC runs. Even if this discontinuity would be better levelled out if many more MC runs were performed, it was checked that the long term evolution used as Reference is reliable and well consistent, also as shown by the comparison with DAMAGE. From the figure we can notice that the simulated scenario has a steady increasing pace with the final population nearly doubled with respect to the initial one. This is due to a significant number of collisional debris added to the environment, as shown in the right panel of Fig. 1, where the green lines shows the number of intact objects as a function of time, the red lines the number of fragments already present in the environment at the 2009 initial epoch and the blue lines the fragments produced during the simulated time span. The solid lines show the results of SDM and the dashed lines the results of DAMAGE, once again showing the very good agreement between the two codes. The steady growth of the fragments shown in Fig. 1 (right panel) is due to a significant number of fragmentations happening in the 200-year time span as shown in the left panel of Fig. 2. In this figure the average number of fragmentations recorded by SDM (blue lines) and DAMAGE (red lines) are shown, along with their $\pm 1\sigma$ curves. It can be noticed how, on average, we can expect 1 collisional fragmentation every 5 years in the Reference scenario. The right panel of Fig. 2 shows the altitude distribution of all the fragmentations recorded in the 50 SDM MC runs. The well known hot spots around 800, 1000 and 1400-1500 km of altitude are clearly visible. This is a first indication that the environment in those particular regions will be heavily perturbed in the future, notwithstanding the possible additional fragmentations artificially introduced in the simulations described in the next Sections. Note that the fragmentations shown in Fig. 2 all involve large targets, up to a few objects in the 8-9 tons range.

It is worth stressing that the situation described above in the Reference scenario can be considered a realistic picture of the future evolution of the debris environment, under the so-called Business-As-Usual assumptions detailed in its definition.

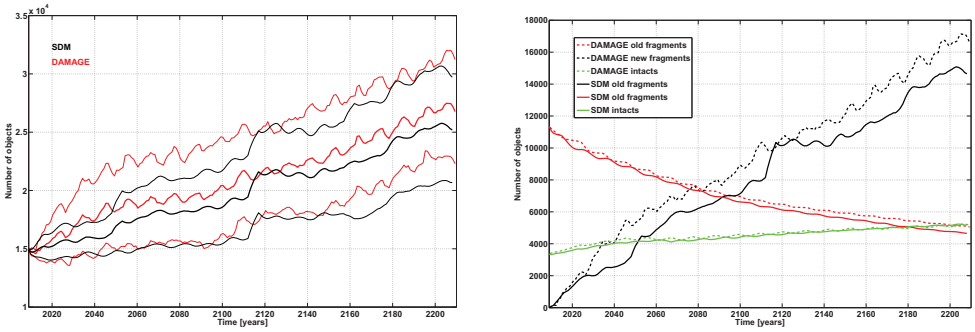

Figure 1: Left panel: average number of objects larger than 10 cm in LEO in the Reference scenario computed with SDM (blue thick line) and DAMAGE (red thick line). The thin lines (of the corresponding colors) show the 1-sigma uncertainty intervals for both codes. Right panel: Breakdown of the population according to the type of objects: the green lines refer to the intact objects, the red line to the fragments already present in the environment at the 2009 initial epoch and the blue line shows the fragments produced during the simulated time span. The solid lines show the results of SDM while the dashed lines show the results of DAMAGE.

3. The LEO fragmentations

A total of 46 fragmentations happening in LEO were simulated. The selected location and the nature of the targets fragmented reflects the actual distribution of the intact objects currently in orbit. A thorough analysis, parametrizing the objects in terms of orbital elements and mass bins, was preliminary conducted to identify the most prominent and representative target objects, identifying a total of 112 orbit-mass bins representing the hot spots of intact object distribution in LEO. A number of filters on size, mass and orbital elements was applied to reduce the number of representative targets. In particular, the cases, in LEO, with inclinations $< 50^\circ$ (a part from the Ariane upper stages) and the objects with mass < 500 kg (with the exception of the Globalstar spacecraft, filling a specific gap in the orbital bin distribution) were excluded. Moreover a coarser resolution in the mass spectra (e.g., merging the bins involving objects with masses differing by less than 30 %) was finally adopted. As a result of this analysis, Tab. 1 lists the first 45 fragmentation events simulated in LEO. All the scenarios of Tab. 1 were simulated with 25 MC runs and the scenarios were repeated twice: one with the fragmentation happening in the year 2020 and another one with the

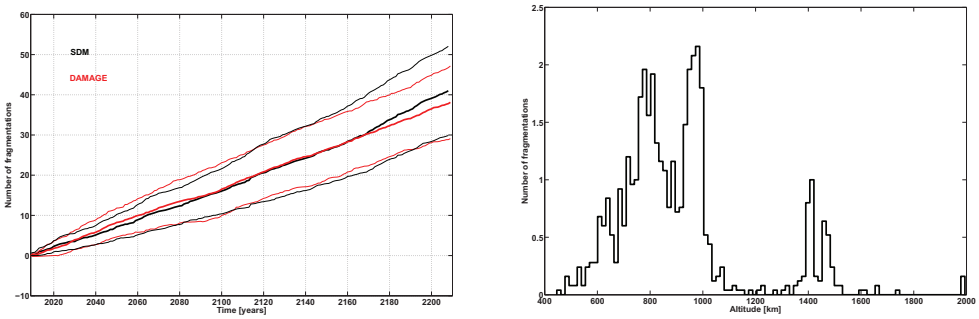

Figure 2: Left panel: average number of catastrophic fragmentations in the Reference scenario. The thick blue line shows the average number of events in the SDM simulations while the thick red line shows the similar results from DAMAGE. The thin lines show the 1-sigma uncertainties. Right panel: altitude distribution of the catastrophic fragmentations recorded in the SDM simulations of the Reference scenario in LEO.

event happening in 2070.

Moreover, since one of the drivers of the present study was the concern for the consequences on the environment of a possible future fragmentation of Envisat, beyond all the events of Tab. 1, the fragmentation of Envisat was also analyzed with particular care. As it is known, after 10 years of fruitful Earth observations, the contacts with the large spacecraft were lost on 8 April 2012 and ESA formally announced the end of Envisat's mission on 9 May 2012. The mass of Envisat is around 8 tons and it is still orbiting in the very crowded region around 750 km of altitude. Due to its altitude, the residual lifetime in orbit is estimated in excess of 100 years. Therefore, there is a significant risk that Envisat could be fragmented upon impact with a debris in the future, creating a large debris cloud. For these reasons a particular set of simulations was devoted to the study of the Envisat case. It was decided to simulate the fragmentation of an Envisat-like spacecraft at four different epochs in the future: in the year 2020, 2045, 2070 and 2095. The fragmentations are simulated along the decaying orbit, that is the orbit of Envisat is propagated for its residual lifetime and each fragmentation is happening at the altitude reached by the spacecraft at the desired epoch. Tab. 2 shows the orbital elements used. The spacecraft mass was assumed to be, in all the epochs, equal to 8050 kg and the fragmentation simulated was due to an impact against a projectile of 6.44 kg travelling at 10 km/sec.

50 MC runs were performed for each scenario.

3.1. Results of the Envisat cases

Figure 3 shows the average number of objects in LEO larger than 10 cm, as a function of time, computed with SDM in 4 different scenarios: the thick blue line shows the Reference scenario results (as in the left panel of Fig. 1, thick blue line), the red line shows the number of objects in the case where the fragmentation of the Envisat-like spacecraft is happening in the year 2020, the magenta line shows the results for the fragmentation happening in the year 2070 and the black line shows the results for the fragmentation happening in the year 2095. The thin blue lines are the $\pm 1\sigma$ curves for the Reference scenario. Figure 4 shows the average number of fragmentations happening in the Envisat scenarios, again compared with the Reference one. It can be noticed how the average number of fragmentations is around 40 over 200 years, with no significant deviations between the Reference and the Envisat fragmentation scenarios. Contrary to what one might expect, the

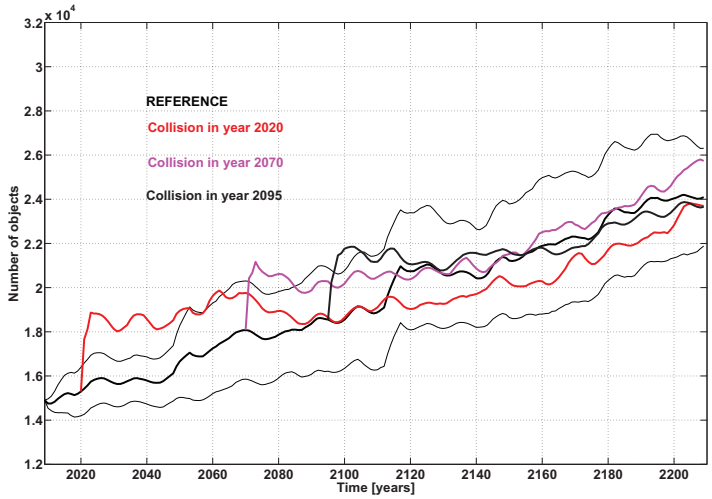

Figure 3: Comparison between the average number of objects larger than 10 cm in LEO in the Reference scenario (thick blue line) with the scenarios where the fragmentation of an Envisat-like spacecraft is simulated in the year 2020 (red line), 2070 (magenta line) and 2095 (black line). The thin blue lines show the $\pm 1\sigma$ interval for the Reference scenario.

final number of objects in all the four cases is statistically the same (i.e., all

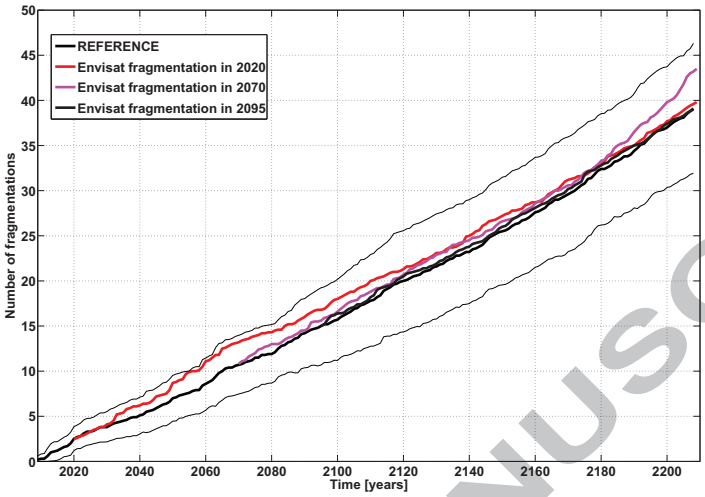

Figure 4: Cumulative number of collisions in the scenarios described in Fig. 3.

well within the $\pm 1\sigma$ standard deviation bounds). From a statistical point of view, the Envisat fragmentations are leading to a long term LEO environment which is indistinguishable from the Reference one. This means that, in the long run, even the fragmentation of a very large spacecraft leaves no noticeable signature on the environment or, in other words, the simulated Envisat fragmentation does not alter, by itself, "permanently" the LEO environment on the long run (200 years). The reason for this outcome is that the reference evolution is highly stochastic and is dominated by a large number of fragmentations (on average one every 5 years). Therefore, the effects of our additional Envisat-like fragmentation get soon "diluted" in the vast number of background fragments and leave almost no trace after 200 years. On the other hand, the situation can be different in the "interim" regime, in the orbital regions in the vicinity of the Envisat fragmentation, during the few decades following the event; these shorter term effects have been studied too and will be described later. Note that the same scenarios described in Fig. 3 were simulated with DAMAGE. The results are again perfectly comparable and are therefore not shown here for sake of conciseness (see (Rossi & Lewis , 2015) for more details on the comparison).

3.2. Results of the LEO cases

Due to lack of space it is impossible to show the results for all the fragmentations listed in Tab. 1. Only some representative results will be displayed and the interested reader can refer to (Rossi & Lewis , 2015) for the complete set of plots. Figure 5 shows the comparison between the average number of objects in LEO in the Reference scenario and for three different scenarios where an 8 ton Zenit-2 R/B in Sun Synchronous Orbit (SSO) is fragmented in the year 2020. In particular, as usual, in the picture, the blue lines refer to the Reference scenario. Then the black line refers to the scenario where the fragmentation happens at an altitude of 639 km, the magenta line to the fragmentation at an altitude of 844 km and, finally, the red line to the fragmentation at 997 km. Similarly, Figure 6 shows the comparison

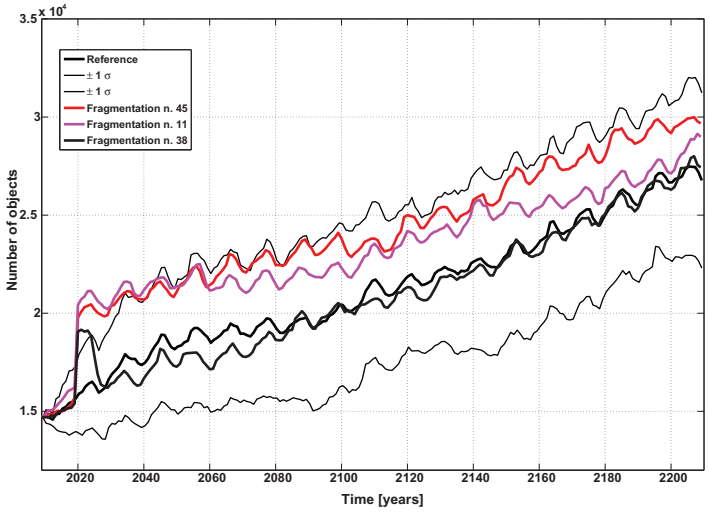

Figure 5: Average number of objects larger than 10 cm in LEO for the fragmentations number 11, 38 and 45, all involving targets of about 8000 kg of mass. The thick blue line shows the Reference scenario and the thin blue lines show the $\pm 1\sigma$ interval for the Reference scenario. The black line shows the evolution for the case of fragmentation number 38 (happening at an altitude of about 639 km), the magenta line for the case 11 (844 km of altitude) and the red line for the case 45 (997 km of altitude).

between fragmentation scenarios with 3 different targets with a mass of 2 tons. In particular, the red lines shows the evolution for the scenario where a COSMO-Skymed satellite, in SSO, is fragmented at an altitude of 623 km,

the black line refers to the scenario with the fragmentation of an Ariane 4 R/B, in SSO, at an altitude of 769 km and the green line to the scenario with the fragmentation of a spacecraft, in SSO, at an altitude of 898 km.

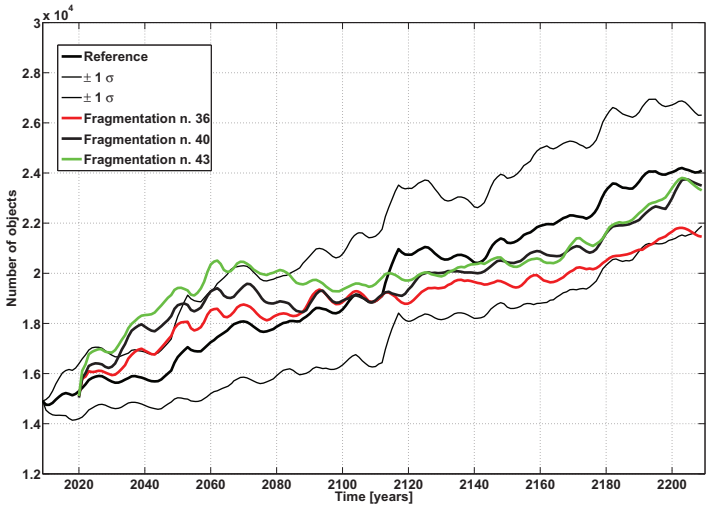

Figure 6: Average number of objects larger than 10 cm in LEO for the fragmentations number 36, 40 and 43, all involving targets of 2000 kg of mass. The thick blue line shows the Reference scenario and the thin blue lines show the $\pm 1\sigma$ interval for the Reference scenario. The red line shows the evolution for the case of fragmentation number 36 (happening at an altitude of about 620 km), the black line for the case 40 (769 km of altitude) and the green line for the case 43 (900 km of altitude).

A first consideration can be made looking at Figs. 5-6: in none of the cases (and this is true also for the other scenarios not shown here; see (Rossi & Lewis , 2015)) the average number of objects in the fragmentation cases, at the end of the investigated time span, lies outside the $\pm 1\sigma$ intervals of the Reference scenario. This means that, statistically speaking, all the events of Tab. 1 are leading to a long term LEO environment which is indistinguishable from the Reference one. In other words, even a large fragmentation on a high LEO is not leaving a strong statistically significant long term signature on the environment. On the other hand, it has to be stressed that this outcome is also related to the large span covered by the $\pm 1\sigma$ curves, which in turns is related to the number of MC runs. Since the $\pm 1\sigma$ curves represent formal uncertainties out of the MC averaging process, the value of σ is decreasing

as the square root of the number of runs. That is, while the displayed results give a reliable statistical indication of the long term evolution, performing a significantly larger number of runs we could limit the $\pm 1\sigma$ intervals and therefore obtain results more sounding from the statistical point of view. Of course, with the large number of simulations foreseen in this study it would have been impossible to increase the number of MC runs to reach this higher level of significance.

Notwithstanding the mentioned caveats, as it will be detailed in the following, some events show long term consequences which can be clearly spotted in the plots and that highlight the driving factors in the environment evolution, which is the main expected output of this study. The first parameter of interest in the simulation is the mass. Again a general consideration can be made here: whenever the mass of the fragmented target is lower than about 1000 kg, no appreciable signature is left on the environment. That is, as stated above even for the much more massive Envisat cases, these kind of events get soon lost in the sea of fragments generated by the other fragmentations.

The largest objects listed in Tab. 1 are the Zenit rocket bodies of cases 11, 38 and 45, with a mass of 8 tons. Looking at Fig. 5 it can be noticed how the consequences of the year 2020 fragmentations are visible in the long term environment of cases 11 and 45, while no signature of the 2020 fragmentation is left in case 38. These differences are clearly related to the altitude of the event. Whereas the fragmentations 11 and 45 happens at high altitudes, respectively at 844 and 997 km, the event number 38 happens more than 200 km below, at 639 km of altitude. The lifetime of the fragments is therefore significantly reduced. These first considerations already point us to the interplay of the most important parameters driving the evolution: mass and altitude. This is also noticeable looking at Fig.6. In this picture the final evolution is comparable in the three cases, with the lowest altitude one (case 36) being slightly lower than the other two. Moreover it can be seen how the effects of the cloud generated in case 36 "expires" much faster than in the other two cases, due to the significantly higher atmospheric drag present around 600 km.

As an example of the interplay between mass and altitude and of the complexity and stochasticity of the problem one can look at Fig. 7, showing the results of the fragmentation of Cosmos-3M R/B on different circular LEO orbits at 771 (red line, fragmentation number 14), 985 (magenta line, fragmentation number 16), 1189 (black line, fragmentation number 18) and 1589 km (green line, fragmentation number 19) of altitude, respectively. In the

first case, with the event happening at 771 km, the Reference and fragmentation scenarios become nearly coincident just a few decades after the collision. This is due to the cleansing effect of the drag on the relatively small debris cloud produced by the moderate mass of the target. A different pattern is noticeable in the magenta line, where the long term evolution of the Reference and fragmentation scenarios follow two parallel and clearly separated tracks, with the signature of the fragmentation apparently visible even after 200 years. This behaviour is clearly dictated by the more than 200 km of difference in altitude with the previous case. Moreover, it is worth noticing that the fragmentation number 16 is happening at the altitude of 980 km, right in the middle of one of the most crowded LEO zone, therefore it is plausible that the added perturbation could generate feedback collisions in the years following the event. Therefore these two events seem to confirm the above conclusions on the role of mass and altitude. Then, the black line shows a similar situation, even if here the onset of the separate track for the fragmentation case appears to be happening only about 40 years after the collision and could be ascribed to other collisions in the region, possibly, but not necessarily, triggered by the perturbed environment produced by the 2020 fragmentation. Also this event, at 1189 km of altitude, is happening close to the densely populated area around 900 km of altitude, so its debris cloud would be interacting in the decades after the event, with a large number of other potential targets. The apparently clear picture just described above is complicated by the results shown by the case of fragmentation number 19 (green line). Here the same mass is fragmented on a significantly higher orbit, but the red and blue lines are almost indistinguishable. A possible explanation here is that, while higher, the event is happening in a much less populated zone so that subsequent feedback collisions are less likely to occur. These latter results point out another important actor in this story, that is the region where the fragmentation takes place, namely in the sense of the spatial density of objects with which the fragments cloud will be interacting. Figure 8, similarly to Fig 7, shows again the average number of objects larger than 10 cm for several scenarios involving the fragmentation of targets with a mass of about 1400 kg, namely the cases 9, 14, 16, 18, 19, 25, 27, 30 and 32. Apart from the Reference scenario (in blue), in this plot all the fragmentation cases are shown with the red lines, except for case 14 (black line), which represents, within the 9 cases considered in the figure, the fragmentation happening on the lowest orbit (at an altitude of 770 km), and case 19 (green line), which represents the fragmentation happening on the

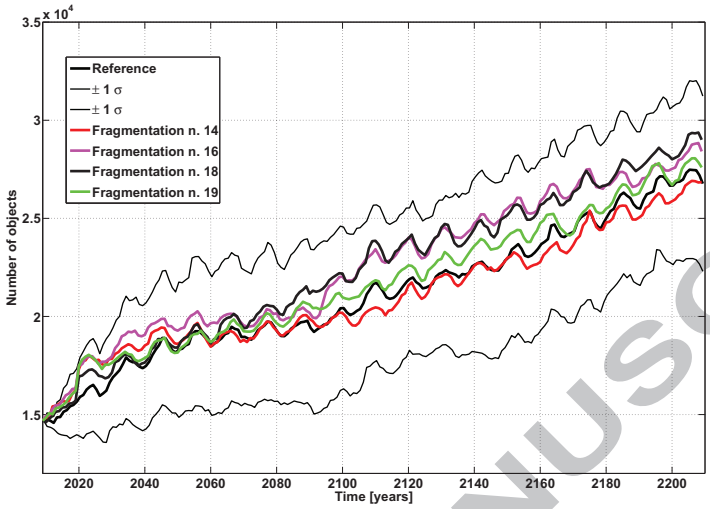

Figure 7: Average number of objects larger than 10 cm in LEO for the fragmentations number 14, 16, 18 and 19, all involving Cosmos R/B of about 1400 kg of mass. The thick blue line shows the Reference scenario and the thin blue lines show the $\pm 1\sigma$ interval for the Reference scenario. The red line shows the evolution for the case of fragmentation number 14 (at an altitude of 771 km), the magenta line refers to the fragmentation number 16 (altitude: 985 km), the black line to the fragmentation number 18 (altitude: 1189 km) and the green line to the fragmentation number 19 (altitude: 1586 km).

highest orbit (at an altitude of 1580). Note that all the cases shown with the red lines refer to fragmentations happening between 950 and 1450 km of altitude, that is on orbits with long residual lifetime. Looking at the plot, it can be noticed how the black line, representing an event happening about 200 km below anyone else, indeed is one of the lowest (but it is not the lowest one). Moreover, clearly all the other cases are either above or below the Reference one, without a clear separation related to the altitude of the event and, in particular, the green line is not on the top of the group. It might be argued that above about 900 km, where the average residual lifetime of the fragments exceeds the investigated time span, the effects of the altitude of the fragmentation, while more important in absolute terms, become less strong as a ranking factor (i.e., it becomes more difficult to anticipate the consequences of an event with respect to a similar one on a different orbit on the basis of their altitude). For sake of completeness, it can be added that

the three top red line lines, above the Reference line, refer to the cases 16, 18 and 25, happening between 950 and 1190 km of altitude, whereas the bottom red line pertains to the case 9, happening at about 980 km of altitude. The only significant difference between the orbits of the targets of case 9 and cases 16, 18 and 25, is that the target of case 9 is on a slightly less inclined orbit, at 65.8 deg, whereas, e.g., the target of case 16 (at nearly the same altitude) is on an orbit with 74 deg of inclination. Although far from conclusive, this might draw our attention to the influence of the inclination on the long term consequences of a fragmentation in LEO. As it is well known, a cloud of debris with near polar inclination will interact with all the orbits in the region, with dangerous crossings close to the poles, thus increasing the overall collision risk.

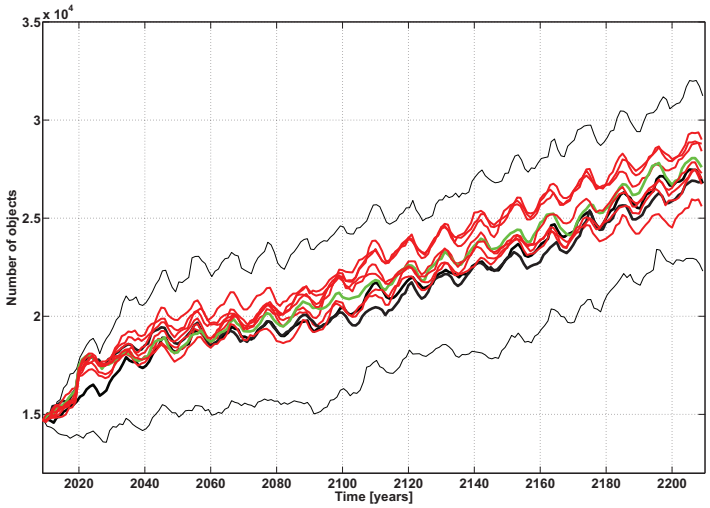

Figure 8: Average number of objects larger than 10 cm in LEO for the fragmentations number 9, 14, 16, 18, 19, 25, 27, 30 and 32, all involving targets of about 1400 kg of mass. The thick blue line shows the Reference scenario and the thin blue lines show the $\pm 1\sigma$ interval for the Reference scenario. The black line shows the evolution for the case of fragmentation number 14 (having the lowest orbit in the selected group, with an altitude of about 770 km) and the green line shows the evolution for the case number 19 (having the highest orbit in the selected group, with an altitude of about 1580 km). All the other cases are shown with red lines, happening in orbits ranging from 950 to 1450 km of altitude.

4. The criticality evaluation norm

In order to properly analyse and highlight the effects of the additional fragmentation events with respect to the underlying reference environment an evaluation norm was introduced. The norm also helps to quantify and easily visualize the results of the simulations. The definition of the norm is as follows.

Given the underlying "Reference" scenario, described in Sec. 2 , and a "fragmentation" scenario in which the simulation of a particular fragmentation is added, the number of objects as a function of time, averaged over all the MC runs is computed for both scenarios. Let $n_{REF}(i)$ be the average number of objects in the Reference scenario and $n_{FRAG}(i)$ the average number of objects in the fragmentation case, in the $i-th$ year. Then, the growth of the population of the "fragmentation" scenario w.r.t. the "Reference" one can be quantified by:

$$C_i = \left(\frac{n_{FRAG}(i) - n_{REF}(i)}{\sigma_{REF}(i)} \right), \tag{1}$$

if $(n_{FRAG}(i) - n_{REF}(i)) \geq 0$, otherwise $C_i = 0$. σ_{REF} is the standard deviation coming from the averaging process over the Monte Carlo runs for the Reference scenario. Whenever $C_i > 1$ the environment is perturbed by the fragmentation event to a level that is above the statistical "noise" of the Monte Carlo runs. As an example, Fig. 9 plots the value of C_i in the case of the Envisat fragmentation scenarios shown in Fig. 3. The decreasing relative importance of the fragmentations happening in later years (due to the larger number of background fragments, to the increase of the value of $\sigma_{REF}(i)$ as a function of time and, mainly, to the lower altitude of the event) is clearly highlighted here. From the values of C_i a ranking of the danger represented by selected fragmentations can be easily expressed with a single number, called C^*. In fact, the sum of the differences, weighted by the time interval, gives an indication of the criticality:

$$C^* = \sum_{i=1}^{N} \frac{C_i}{N} \tag{2}$$

where N is the number of years in the simulation. In the next Sections the application of the C^* norm to the investigated scenarios will be shown.

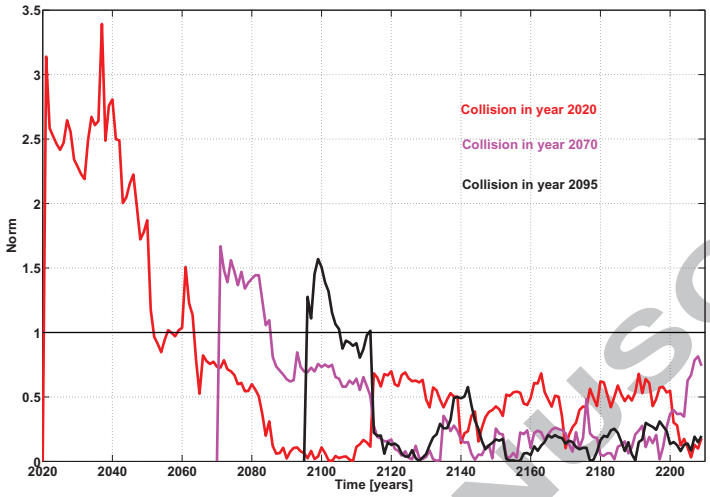

Figure 9: The time evolution of the norm of Eq. 1, computed for the three Envisat-like fragmentations, shown in Fig. 3.

4.1. The LEO cases C^* evaluation

A classification of all the fragmentation events simulated can be performed using the criticality evaluation norm, C^*, described in Sec. 4.

Note that the two sets of simulations (SDM and DAMAGE) had to be kept separated since the computation of C^* depends on the value of the standard deviation, σ_{REF} , of the Monte Carlo process, so each model must be processed coherently with its own σ_{REF} . That is, being model dependent, the C^* values have to be considered as relative evaluations of the effect of a given fragmentation within each model.

The relation between the C^* and the physical and orbital parameters of the fragmented objects can be plotted to highlight the main factors driving the long term evolution.

In particular the plots in Figs. 10 show the relation between the C^* values and the mass and altitude of the fragmented objects for the cases simulated with SDM. The results are fitted with a simple linear relation of the form: $f(x) = ax + b$. The linear fit clearly visualizes the growing trend as a function of mass and altitude of the target. It can be noticed how the data are quite dispersed around the linear fit (and this is reflected in the classical

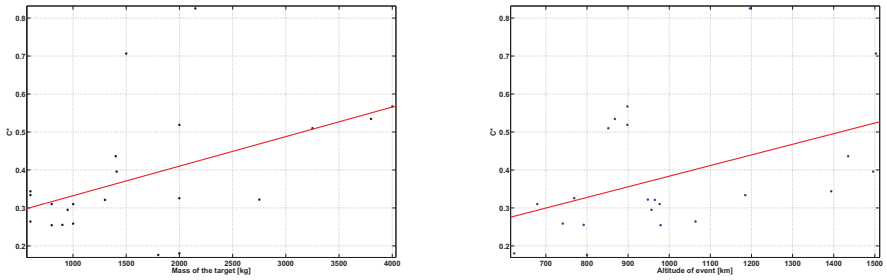

Figure 10: Linear fit of the C^* values as a function of the mass (left panel) and altitude (right panel) of the fragmentation, for the cases simulated with SDM.

indicator of the goodness of the fit, such as the summed square of residuals, the sum of squares of the regression, etc). In particular, the relation with the inclination (not shown here) is poorer than with the other two parameters. Beyond the variability mentioned above, this is related to the fact that, as already mentioned, it is actually a combination of the different parameters that drives the evolution. In fact the situation improves significantly if the fit is attempted for a plot where the relation between a linear combination of the parameters and the C^* is considered. In particular, Fig. 11 shows the relation between C^* and the product of the altitude of the fragmentation by the mass of the target (normalized to 10000 kg for ease of visualization) and by a function of the inclination, $\Gamma = [(1 - \cos(i))/2]$. In this case the linear fit still shows a trend similar to that of Fig. 10, but with significantly better (almost doubled) goodness indicators. It is worth noting that the addition of the inclination function Γ to the fit does not improve the level of the fit, giving a further indication that, on the long term, the initial inclination of the target is playing a minor role.

The DAMAGE plots show similar results and are not included since they are not adding significant information to what was described above.

5. LEO cases: short term analysis

In the previous sections the focus was on the long term effects of a given fragmentation. As already mentioned, only a few specific events leave a significant signature on the long term evolution of the overall population. This, of course, does not mean that the simulated fragmentations have no

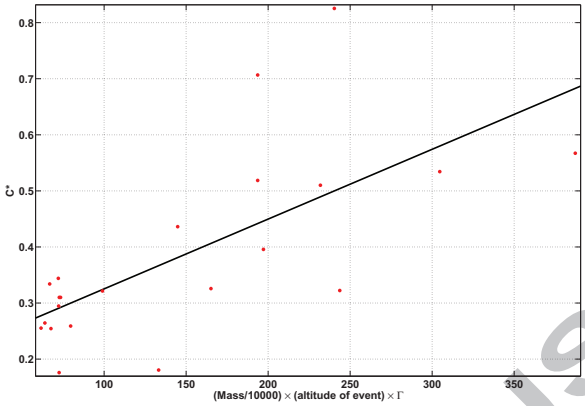

Figure 11: Linear fit of the C^* values as a function of the mass of the target (normalized to 10000 kg) multiplied by the altitude of the fragmentation and the inclination function Γ (see text for details), for the cases simulated with SDM.

consequences on the environment and in particular on the orbital zone around the altitude of the event. That is, in the transient period before the fragments coming from the forced fragmentation, get "absorbed" by the background fragments produced by other collisions, the spatial density of objects in the vicinity of the orbit of the target is significantly increased, thus leading to possible feedback collisions and, certainly, to dangerous crossings with the operational spacecraft in that region. As an example, Figs. 12-13 show the spatial density of objects as a function of time, around the altitude of the fragmentation, for three events from Tab. 1. The left panel of Fig. 12 shows the time evolution of the spatial density of objects larger than 10 cm in the altitude shell between 900 and 1000 km, for the case number 24 in Tab. 1, namely a Meteor-2 spacecraft with a mass of 2750 kg, fragmented in the year 2020 at an altitude of 948 km. The right panel of Fig. 12 is instead showing the same quantity, in the altitude shell between 850 and 950 km of altitude, for the case number 44 in Tab. 1, namely a Sun Synchronous spacecraft with a mass of 4000 kg, fragmented in the year 2020 at an altitude of 898 km.

Figure 13 shows the same quantity, in the altitude shell between 1150 and 1250 km of altitude, for the case number 26 in Tab. 1, namely a Meteor 3 spacecraft with a mass of 2150 kg, fragmented in the year 2020 at an altitude of 1196 km.

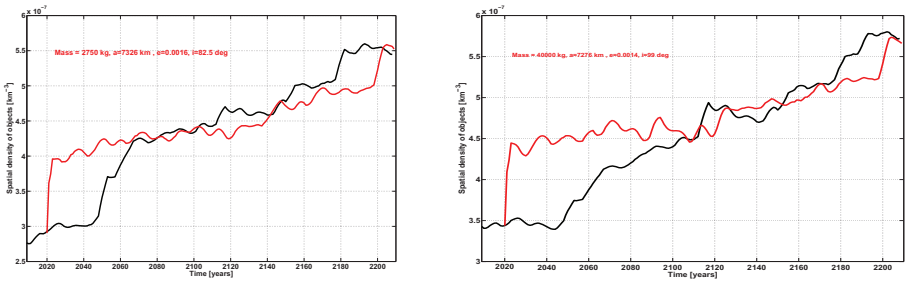

Figure 12: Left panel: spatial density of objects larger than 10 cm as a function of time for the fragmentation number 24 (red line) with respect to the Reference scenario (blue line). Right panel: the same quantity as in the left panel, for the fragmentation number 44.

Looking at the plots it is clear how in the highest shell the density remains actually significantly above the reference level throughout the simulation time span, due to the added fragmentation of the large Meteor-3 spacecraft. Lowering the altitude of the event, in Fig. 12, it can be noticed how the "local" environment in the vicinity of the target orbits still remains highly perturbed for a timespan between 40 to 80 years. This analysis of the short term effects highlights the fact that, even if it might be inconsequential on the overall long term evolution of the whole LEO environment, a massive fragmentation perturbs the local situation around the original target orbit thus jeopardizing all the spacecraft orbiting in that region. Further analysis of the local short term consequences of the simulated fragmentations would certainly deserve additional efforts in the future.

6. The GEO cases

Table 6 summarizes the fragmentation events simulated in GEO. For each one of the events in the list, a scenario with the fragmentation happening in the year 2020 and a scenario with the fragmentation happening in the year 2070 were simulated. For each scenario 25 MC runs were performed. In this section we will summarize the results of the simulations, concentrating on the most significant events. In the following we will refer to each event with the identification number listed in the first column of Tab. 6. Figs. 14-15 show the average effective number of objects larger than 10 cm in the GEO region for some of the scenarios of Tab. 6. The thick blue line shows the number of

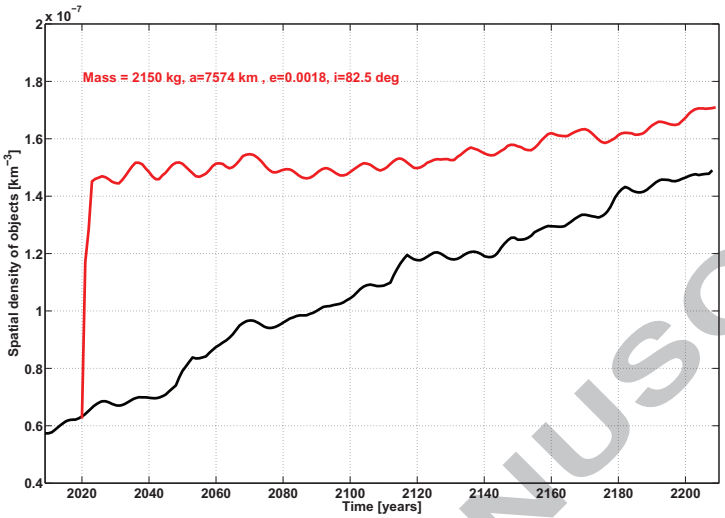

Figure 13: Spatial density of objects larger than 10 cm as a function of time for the fragmentation number 26 (red line) with respect to the Reference scenario (blue line).

objects in the Reference scenario, described in Sec. 2, while the thin blue lines show the $\pm 1\sigma$ intervals of the MC runs of the Reference scenario. Fig. 14 shows the comparison between the Reference scenario and the cases where a 1000 kg spacecraft is fragmented in the year 2020 on an operational orbit (case number 1, red line), in an inclined orbit at the GEO altitude (abandoned object of case 5, magenta line) and in an inclined graveyard orbit (case 11, black line). Similarly, Fig. 15 shows the comparison between the Reference scenario and the cases where a 3000 kg spacecraft is fragmented in the year 2020 on an operational orbit (case number 2, red line), in an inclined orbit at the GEO altitude (abandoned object of case 6, magenta line) and in an inclined graveyard orbit (case 12, black line). As an example of the influence of the epoch of the fragmentation, Fig. 15 shows the comparison between the Reference scenario (blue line) and the cases where a 3000 kg spacecraft is fragmented, in a GEO graveyard orbit with an equatorial inclination of 7.5° (case 10 of Tab. 6), either in the year 2020 (red line) or in the 2070 (black line). As a general comment, it can be noticed how the situation appears clearly different here with respect to the LEO cases. Due to the lower background population and to the lower number of fragmentation events in the

Reference scenario, a massive collisional fragmentation, either in the year 2020 or 2070, is altering the GEO environment indefinitely. On the other hand, it should be noted that, in all the cases involving a fragmentation of a 1000 kg spacecraft, the evolution remains well within the $\pm 1\sigma$ intervals of the Reference scenario. In fact, also in all the 50 MC runs of the Reference, on average, about 1.5 fragmentations (involving a large target between 2000 and 6000 kg of mass) are happening in the investigated GEO region. In the cases where the fragmentation of a 3000 kg spacecraft is simulated, the long term evolution of the fragmentation cases of Tab. 6 lies at the upper border of the $\pm 1\sigma$ curve, but still mostly below it. It is worth stressing that in the long term evolution no relation with the initial orbit of the target (i.e., altitude above the GEO ring and inclination) is detectable. That is, for the GEO cases, the driving factor seems to be just the target mass. Moreover, moving the epoch of the event from 2020 to 2070 does not change the overall characteristics of the long term evolution.

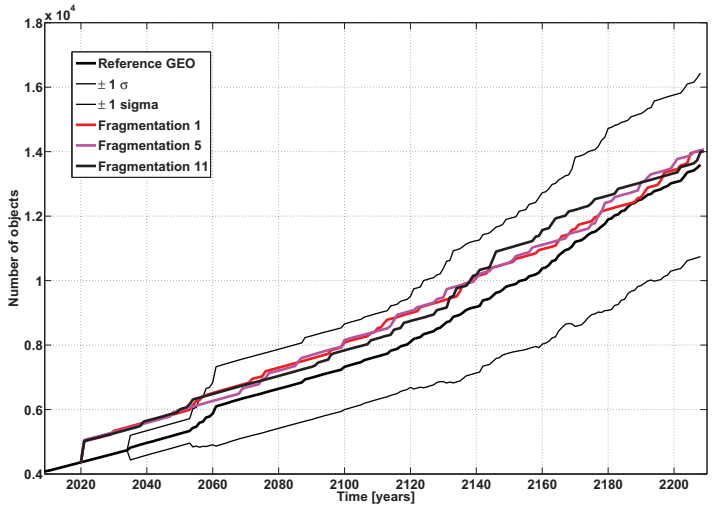

Figure 14: Average number of object in the GEO region for the Reference scenario (thick blue line) compared with the cases number 1 (red line), number 5 (magenta line) and number 11 (black line) of Table 6 (see text for details). The thin blue lines represent the $\pm 1\sigma$ intervals of the Monte Carlo runs.

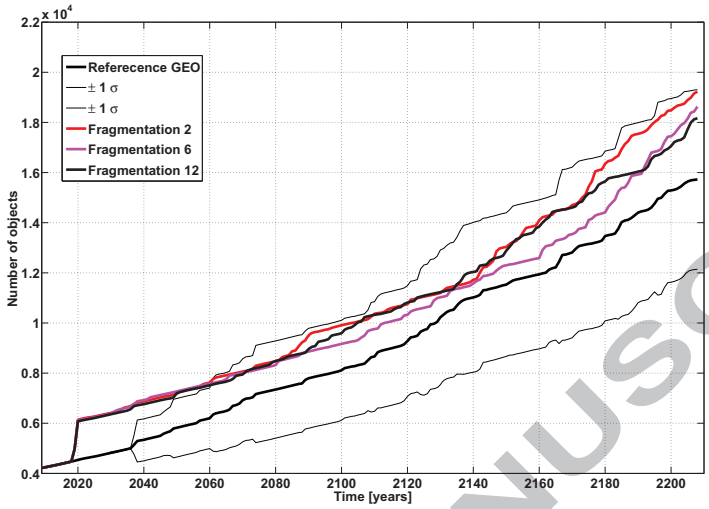

Figure 15: Average number of object in the GEO region for the Reference scenario (thick blue line) compared with the cases number 2 (red line), number 6 (magenta line) and number 12 (black line) of Table 6 (see text for details). The thin blue lines represent the $\pm 1\sigma$ intervals of the Monte Carlo runs.

7. Conclusions

The long term simulations of the LEO environment perturbed by the collisional fragmentation of large objects allowed us to highlight the main factors determining the environmental consequences associated with a given collision event. First, as a general conclusion, it can be stated that, due to the highly stochastic evolution of the LEO environment, even the fragmentation of a massive spacecraft might not be able to alter the long term evolution of the LEO population beyond the intrinsic statistical variability associated with the Monte Carlo procedure. On the other hand, thanks to the performed simulations, some parameters determining the long term effects of a fragmentation in LEO were identified. First the mass and the altitude of the event play a paramount role. It is actually a combination of these two factors, altitude and mass, that is driving the long term effects of a fragmentation in LEO. The orbital inclination is playing a minor role in this picture, with higher inclination targets slightly more prone to give rise to more visible long term effects. The very large number of simulations performed certainly

helped to add quantitative arguments to the a-priori intuitive hypothesis about the importance of mass and orbital altitude of the fragmented targets in the long term evolution of the LEO debris population.

The situation is different in the GEO region. The lower number of background objects and the reduced number of stochastic collisions (on average about 1.5 over 200 years) makes the growth of objects any additional fragmentation much more significant than in LEO. The addition of a massive fragmentation lives a signature on the environment that is detectable throughout the investigated time span. In the case of the GEO simulation the only factor important to asses the long term consequences of a fragmentation appears to be the mass of the target. Events happening in the GEO ring, or in inclined orbit at the GEO altitude (abandoned objects) or in a disposal orbit above the ring produce similar long term evolutions. The evaluation norm described in the paper allows to highlight the differences between comparative long term evolution scenarios and offers a quantitative measure of the effects of specific parameters affecting the evolution.

It is worth stressing at this stage that from the analysis of the simulations it clearly came out that, although the obtained results are certainly sounding, interesting and quantitatively new, a higher number of MC runs for each scenario would have lead to a better statistical significance of the results. Building on the experience gained in this work, it would be desirable, in future studies, to concentrate on a smaller number of highly significant events (mass larger than ~ 1000 kg and altitude above ~ 800 km) with a number of MC runs in excess of 100.

Acknowledgements

The study described in the paper was performed in the framework of the contract: *Assessment Study for Fragmentation Consequence Analysis for LEO and GEO Orbits*, ESA/ESOC No. 4000106534/12/F/MOS. Part of this research was performed in the framework of the FP7-PEOPLE-2012-ITN: *Stardust - The Asteroid and Space Debris Network*. The authors wish to thank the anonymous referees for their comments that helped to improve the paper.

References

Lewis, H.G., White, A.E., Crowther, R., Stokes, H., 2012. Synergy of debris mitigation and removal. Acta Astronautica, 81, 62 – 68.

Liou J.-C., Rossi, A, Krag, H., Raj, X.J., Anilkumar, A.K., Hanada, T., Lewis, H.G., 2013. Stability of the future LEO environment, Inter-Agency Space Debris Co-ordination Committee, AI 27.1 Report, IADC-12-08, available at <http://www.iadc-online.org>.

Rossi, A., Anselmo, L., Pardini, C., Jehn, R., Valsecchi, G.B., 2009. The new Space Debris Mitigation (SDM 4.0) long term evolution code. In: Proceedings of the Fifth European Conference on Space Debris, ESA SP-672, CD-ROM, ESA Communication Production Office, Noordwijk, The Netherlands.

Rossi, A. and Lewis, H., 2015. The long-term environment evolution results, Version 1.0, Study Note for the Contract: "Assessment Study for Fragmentation Consequence Analysis for LEO and GEO Orbits", ESA/ESOC No. 4000106534/12/F/MOS.

	Proj. Mass [kg]	Target Mass [kg]	Inc. [deg]	a [km]	Ecc.	RAAN [deg]	Arg. perig. [deg]	True Anom. [deg]	Altit. [km]	Type
1	1.44	1800	7.0	22468	0.7036	270	205.0	34.4	800	Ariane 4 R/B
2	2.88	3600	5.0	24445	0.7167	100	200.0	23.7	801	Ariane 5 R/B
3	0.28	350	52.0	7792	0.0003	252	8.0	90.0	1414	Globalstar
4	1.12	1400	56.1	7813	0.0096	113	319.0	90.6	1435	Cosmos-3M R/B
5	1.20	1500	63.0	26574	0.7334	0	280.0	14.2	800	Molniya
6	1.04	1300	65.0	7343	0.0030	60	74.0	90.2	965	US-A (RORSAT)
7	1.00	1250	65.0	26563	0.7034	0	270.0	0.0	1500	US-K Oko
8	0.76	950	65.8	7335	0.0012	35	73.0	90.1	957	DS-P1-M (Lira)
9	1.12	1400	65.8	7354	0.0063	63	270.0	90.4	976	Cosmos-3M R/B
10	2.60	3250	71.0	7230	0.0008	151	167.0	95.3	852	Tselina-2
11	6.64	8300	71.0	7222	0.0014	254	0.0	90.1	844	Zenit-2 R/B
12	1.20	1500	73.6	7881	0.0029	223	139.0	91.4	1503	GEO-IK (Musson)
13	0.72	900	74.0	7170	0.0015	29	58.0	90.1	792	Strela-2M
14	1.12	1400	74.0	7149	0.0017	4	277.0	90.1	771	Cosmos-3M R/B
15	0.64	800	74.0	7357	0.0023	164	78.0	90.1	979	Tsiklon
16	1.12	1400	74.0	7363	0.0020	224	179.0	90.1	985	Cosmos-3M R/B
17	0.48	600	74.0	7772	0.0039	67	335.0	90.1	1394	Sfera
18	1.12	1400	74.0	7567	0.0034	131	23.0	90.1	1189	Cosmos-3M R/B
19	1.12	1400	74.0	7964	0.0133	123	236.0	90.8	1586	Cosmos-3M R/B
20	1.40	1750	81.2	6979	0.0014	320	198.0	90.1	601	Tselina-D
21	3.04	3800	81.2	7246	0.0039	302	63.0	90.1	868	Meteor-1
22	2.20	2750	81.2	7237	0.0025	341	99.0	90.1	859	Meteor-2
23	1.07	1340	81.2	7231	0.0089	92	87.0	90.5	853	Vostok R/B
24	2.20	2750	82.5	7326	0.0016	199	112.0	90.1	948	Meteor-2
25	1.13	1410	82.5	7326	0.0014	31	309.0	90.1	948	Tsiklon-3 R/B
26	1.72	2150	82.5	7574	0.0018	187	170.0	90.1	1196	Meteor-3
27	1.12	1410	82.5	7614	0.0016	31	262.0	90.1	1236	Tsiklon-3 R/B
28	1.13	1410	82.5	7874	0.0008	215	169.0	90.1	1496	Tsiklon-3 R/B
29	0.64	800	83.0	7355	0.0026	45	356.0	90.1	977	Tsiklon
30	1.12	1400	83.0	7347	0.0042	344	143.0	90.1	969	Cosmos-3M R/B
31	0.48	600	83.0	7563	0.0036	250	339.0	90.1	1185	Sfera
32	1.12	1400	83.0	7568	0.0053	282	88.0	90.3	1190	Cosmos-3M R/B
33	0.56	700	86.4	7156	0.0003	328	78.0	90.0	778	Iridium
34	0.48	600	90.0	7442	0.0056	320	306.0	90.3	1064	Able-Star R/B
35	0.80	1000	98.0	7057	0.0009	112	212.0	90.1	679	GeoEye-1
36	1.60	2000	98.0	7001	0.0001	223	76.0	90.1	623	COSMO-Skymed
37	3.20	4000	98.0	7053	0.0001	113	163.0	90.1	675	Helios-2
38	6.40	8000	98.0	7017	0.0016	359	179.0	90.1	639	Zenit-2 R/B
39	0.80	1000	98.5	7119	0.0143	291	307.0	90.8	741	Delta 2 R/B
40	1.60	2000	98.5	7147	0.0011	21	43.0	90.1	769	Ariane 4 R/B
41	3.20	4000	98.5	7158	0.0014	9	274.0	90.1	780	SSO S/C & R/B
42	0.80	1000	99.0	7233	0.0015	339	83.0	90.1	855	NOAA-19 in SSO
43	1.60	2000	99.0	7276	0.0014	16	118.0	90.1	898	SSO S/C & R/B
44	3.20	4000	99.0	7276	0.0014	90	156.0	90.1	898	SSO S/C & R/B
45	6.40	8000	99.0	7375	0.0016	222	153.0	90.1	997	Zenit-2 R/B

Table 1: List of the simulated LEO collisional fragmentations.

Epoch	Semimajor axis [km]	Eccentricity	Inclination [deg]
2020	7137	0.0011	98.2
2045	7121	0.0001	98.4
2070	7099	0.0001	98.6
2095	7073	0.0013	98.4

Table 2: Orbital elements of the fragmented Envisat-like spacecraft

	Proj. Mass [kg]	Target Mass [kg]	Inc. [deg]	a [km]	Ecc.	RAAN [deg]	Arg. of perigee [deg]	True Anom. [deg]	Altitude [km]	Type
1	125	1000	0.1	42164	0.0005	85.0	235.0	125.0	35798	O
2	375	3000	0.1	42164	0.0005	265.0	64.0	296.0	35777	O
3	125	1000	7.5	42164	0.0030	56.0	288.0	72.0	35746	A
4	375	3000	7.5	42164	0.0030	310.0	23.0	337.0	35669	A
5	125	1000	15.0	42164	0.0030	0.0	90.0	270.0	35785	A
6	375	3000	15.0	42164	0.0030	0.0	270.0	90.0	35785	A
7	125	1000	0.1	42600	0.0030	265.0	49.0	311.0	36138	R
8	375	3000	0.1	42600	0.0030	85.0	200.0	160.0	36342	R
9	125	1000	7.5	42600	0.0030	310.0	290.0	70.0	36178	R
10	375	3000	7.5	42600	0.0030	56.0	14.0	346.0	36098	R
11	125	1000	15.0	42600	0.0030	0.0	270.0	90.0	36221	R
12	375	3000	15.0	42600	0.0030	0.0	90.0	270.0	36221	R

Table 3: List of all the simulated GEO fragmentations. All the fragmented objects are GEO spacecraft, either operational (O), abandoned (A) or re-orbited (R) above the ring.